Şöhretoğlu D, Barut B, Sari S, Özel A, Arroo R (2020) In vitro and in silico assessment of DNA interaction, topoisomerase I and II inhibition properties of chrysosplenetin. International Journal of Biological Macromolecules 163: 1053-1059.
https://doi.org/10.1016/j.ijbiomac.2020.07.049

In vitro and *in silico* assessment of DNA interaction, topoisomerase I and II inhibition properties of Chrysosplenetin

Didem Şöhretoğlu[a*], Burak Barut[b], Suat Sari[c], Arzu Özel[b,d], Randolph Arroo[e]

[a] Hacettepe University, Faculty of Pharmacy, Department of Pharmacognosy, Sıhhiye, Ankara, TR-06100, Ankara, Turkey

[b] Karadeniz Technical University, Faculty of Pharmacy, Department of Biochemistry, Trabzon, Turkey

[c] Hacettepe University, Faculty of Pharmacy, Department of Pharmaceutical Chemistry, Sıhhiye, Ankara, TR-06100, Ankara, Turkey

[d] Karadeniz Technical University, Drug and Pharmaceutical Technology Application and Research Center, Trabzon, Turkey

[e] De Montfort University, Leicester School of Pharmacy, The Gateway, Leicester, LE1 9BH, United Kingdom

*Corresponding author: didems@hacettepe.edu.tr

Abstract

Chrysosplenetin is a methoxyflavone with reported anti-cancer effect. We tested its cytotoxic effect on the MCF-7 breast cancer cell line, and determined its effect on DNA intercalation and on the activity of topoisomerases I and II. The compound inhibited proliferation MCF-7 with an IC_{50} value of 0.29 µM. Chrysosplenetin did not initiate plasmid DNA cleavage but, in a concentration-dependent manner, protected plasmid DNA against damage induced by Fenton reagents. Furthermore, it possessed dual Topoisomerase I and II inhibitory properties. Especially, it inhibited topoisomerase II by 83-96% between the range 12.5-100 µM. In the light of these experimental findings, molecular docking studies were performed to understand binding mode, interactions and affinity of chrysosplenetin with DNA, and with topoisomerases I and II. These studies showed that of 4-chromone core and the hydroxyl and methoxy groups important for both intercalation with DNA and topoisomerase I and II inhibition.

Keywords: Chrysosplenetin, DNA, topoisomerase, flavonol, flavonoid

1. Introduction

Chrysosplenetin, (3,6,7,3'-tetra-methylquercetagetin) is a polymethoxylated flavone found in some Asteraceae plants like *Chamomilla recutita* (L.) Rauschert and *Artemisia annua* L. [1, 2]. Reportedly, this compound enhances osteoblastogenesis in human bone marrow stromal cells and suppresses postmenopausal osteoporosis in mice [3] It also inhibits the activity of tyrosinase [4] and neuraminidase [5] and has antimicrobial properties [6, 7]. Furthermore, it selectively inhibits proliferation of breast cancer cell lines MDS-MB-231, MCF-7 and T47D, while having comparatively little toxic profiles on normal non-tumour cells (e.g. MRC-5 and HUVEC) [7, 8]. Proposed mechanism of action involves triggering PI3K/Akt signaling pathway-associated apoptosis, or activating the mitotic spindle checkpoint which alters microtubule depolymerization and also results in apoptosis [9].

Topoisomerases are enzymes that play a crucial role in DNA replication, recombination, transcription and repair [10]. Based on their reaction mechanism, catalytic function, and amino acid sequence and consequent tertiary structure, two types of topoisomerase are distinguished in humans: topoisomerase I and II [11]. Topoisomerase I acts by cleaving one DNA strand, whereas topoisomerase II breaks two strands. Topoisomerase I shows both nuclease and ligase activities. The energy released by hydrolysis of the phosphodiester bonds during nuclease activity is stored, and used later when the strand is ligated again. Therefore, there is no ATP requirement. In contrast, during the ligase activity of the two strands for topoisomerase II, ATP is needed [12]. Many studies have shown that certain cancer cells have high level of topoisomerase expression. Thus, topoisomerase inhibitors have been widely investigated in the development of new anticancer compounds. Daunorubicin, mitoxantrone, teniposide, etoposide, irinotecan and topotecan are used as topoisomerases inhibitors for cancer treatment in clinic despite severe adverse effects including

cardiotoxicity, immune system depression, tremor, and fever [13, 14] Therefore, there is a need for novel topoisomerase inhibitors with significantly reduced toxicity profiles.

Flavonoids are the most common group of polyphenolic compounds in human diet. It is widely accepted that the dietary flavonoids in fruits and vegetables play a key role in prevention of diseases such as cancer [15, 16]. In addition, some flavonoids exhibit anticancer properties through different mechanisms including topoisomerase I and II inhibition [11]. Notably, some of them were found to be stronger topoisomerase II inhibitor than etoposide [17]. Taking into account the highly promising anticancer properties of chrysosplenetin, we aimed to investigate its interactions with DNA, and its inhibitory effects on topoisomerase I and II, through *in vitro* and *in silico* studies.

2. Materials and methods

2.1. Materials and reagents

Chrysosplenetin, isolated from *Artemisia annua* L., was a gift from Botanical Developments Ltd (Maidstone, UK), >95% purity was confirmed by HPLC-DAD and ^{1}H-NMR. Acetic acid, agarose, adenosine 5'-triphosphate disodium salt hydrate (ATP), bovine serum albumin (BSA), bromophenol blue, dithiothreitol (DTT), ethylenediaminetetraacatate (EDTA), ethidium bromide (EB), glycerol, hydrochloric acid (HCl), hydrogen peroxide (H_2O_2), iron (II) sulfate ($FeSO_4$) magnesium chloride ($MgCl_2$), potassium chloride (KCl), sodium dodecyl sulfate (SDS), spermidine, trisma-base (Tris), and xylene cyanol were purchased from Sigma. Supercoiled pBR322 plasmid DNA was obtained from Fermantas and topoisomerase I/II enzymes were purchased from Topogen. Fetal calf serum (FCS), trypsin–EDTA, Dulbecco's modified Eagle's medium (DMEM), penicillin-streptomycin, and L-glutamine were purchased from Biological

Industries (Kibbutz Beit-Haemek, Israel); dimethyl sulfoxide from Sigma, and MTS Cell Proliferation Assay kit from Promega (USA). The DNA cleavage/protective and topoisomerases inhibition studies were visualized using BioRad Gel Doc XR system. The results were calculated using Image Lab Version 4.0.1 Software program.

2.2. Cytotoxic effects

Cytotoxic effects of chrysosplenetin on MCF-7 cell line was evaluated by MTS assay, using CellTiter 96 Aqueous One Solution Cell Proliferation Assay kit (Promega), according the manufacturer's instructions. Briefly, cells suspended in the growth medium were seeded in a 96-well plate at a density of 10,000 cells per well. Following a 24-h incubation, chrysosplenetin (0–10 mM) was added. After incubation for 72 h, 20 ml solution reagent was added to each well and the cells were incubated for an additional 1 h. Cell proliferation was determined at 490 nm using a UV-VIS spectrophotometer (Bio-Tek Instruments, M-Quant Biomolecular spectrophotometer). Cells treated with vehicle alone served as control. The test was repeated three times [18].

2.3. *Supercoiled pBR322 plasmid DNA hydrolytic cleavage experiments*

The supercoiled pBR322 plasmid DNA (Thermo Scientific, SD0041) hydrolytic cleavage activity of chrysosplenetin was examined using agarose gel electrophoresis (Bio-Rad, Wide Mini-Sub Cell GT Cell). In this work, the stock solution of chrysosplenetin at 10 mM was prepared in DMSO and diluted to working solutions (12.5, 25, 50, 100 and 200 μM) with buffer (50 mM Tris-HCl (pH 7.0)). Control experiments were done in the presence of DMSO (2%). Chrysosplenetin was treated with supercoiled pBR322 plasmid DNA at 37 °C for 1 h in the buffer. After incubation, loading buffer (bromophenol blue, xylene cyanol, glycerol, EDTA, SDS) was added and the reaction mixtures were loaded on agarose gel (0.8%) with EB staining for 90 min at 100 V in TAE

(Tris-acetic acid-EDTA) buffer. After electrophoresis, band intensities were photographed and calculated using BioRad Gel Doc XR system and Image Lab Version 4.0.1 Software program [19].

2.4. *Supercoiled pBR322 plasmid DNA protective experiments*

The supercoiled pBR322 plasmid DNA protective effects of chrysosplenetin against oxidative damage of hydroxyl radicals from Fenton reaction were examined using agarose gel electrophoresis according to our previously studies [20]. In this work, the reaction mixture containing Tris-HCl (pH 7.0), supercoiled pBR322 plasmid DNA, $FeSO_4$ (1 mM), H_2O_2 (2%), and different concentrations of chrysosplenetin (12.5, 25, 50 and 100 μM) were incubated at 37 ºC for 1 h. The electrophoresis experiments were performed according to the method detailed above.

2.5. *Topoisomerase I and II inhibition assay*

Topoisomerase inhibition assays of chrysosplenetin were performed as described in our previously studies with slight modifications [21]. Control experiments were done in the presence of DMSO (2%). Briefly, 1 unit of human topoisomerase I (Topogen, TG2005H-RC1) and supercoiled pBR322 plasmid DNA was treated with or without chrysosplenetin (12.5, 25, 50 and 100 μM) in relaxation buffer including Tris-HCl (pH 8.0), BSA, DTT, KCl, $MgCl_2$, and spermidine for 1 h at 37 ºC. After incubation, loading buffer (bromophenol blue, xylene cyanol, glycerol, EDTA, SDS) was added to the reaction mixture. The reaction mixtures were loaded on agarose gel (0.8%) with EB staining for 180 min at 40 V in TAE buffer. After electrophoresis, band intensities were photographed and calculated using BioRad Gel Doc XR system and Image Lab Version 4.0.1 Software program.

In topoisomerase II inhibition assay, 1 unit of human topoisomerase II (Topogen, TG2000H-1) and supercoiled pBR322 plasmid DNA was treated with or without chrysosplenetin (12.5, 25,

50 and 100 µM) in relaxation buffer including Tris-HCl (pH 8.0), ATP, BSA, DTT, KCl, $MgCl_2$, and spermidine for 1 h at 37 ºC. The electrophoresis experiments were performed according to the method detailed above.

2.6. *Molecular docking studies*

Chrysosplenetin and the co-crystallized ligands were modelled and optimized by MacroModel (2019-4: Schrödinger, LLC, New York, NY) using OPLS3e forcefield (2019-4: Schrödinger, LLC, New York, NY) and conjugate gradient algorithm [22]. Using AutoDockTools (v1.5.7, The Scripps Research Institute, San Diego, CA) [23], the ligands were prepared for docking by treating bond orders, hydrogens and adding partial charges (Gasteiger) and converted to the pdbqt format. Selected 20 DNA structures (PDB ID: 3AJK [24], 3OIE [25], 3U0U [26], 3U05 [26], 4AH0 [27], 4IJ0 [28], 4U8B [29], 4U8C [29], 6AST [30], 6GIM [31], 1N37 [32], 1Z3F [33], 2DES [34], 2MG8 [35], 3FT6 [36], 4BZT [37], 182D [38], 198D [39], 224D [40], 367D [41]) and human topoisomerase I (PDB ID: 1K4T [42]) and II (PDB ID: 3QX3 [43]) in covalent complex with DNA were downloaded from the RCSB Protein Data Bank (www.rcsb.org) [44]. The macromolecules were prepared using AutoDockTools by removing unwanted residues and chains, assigning bond orders, adding hydrogens and Gasteiger charges, and ultimately, saving in pdbqt format. Grid maps were generated using AutoGrid (v4.2, Scripps Research Institute, San Diego, CA) [23] taking the central coordinates of the co-crystallized ligand for each pdb structure with 60 grid points for each dimension and 0.375 Å spacing. Chrysosplenetin was docked to each macromolecule using the prepared Grid maps and AutoDock (v4.2, Scripps Research Institute, San Diego, CA) [23] with the following settings: Lamarckian genetic algorithm was selected, genetic algorithm search parameters were set as 2,500,000 for maximum number of evaluations and 150 as population size, and each ligand was docked 50 times to each macromolecule. The docking score

(energy of free binding, kcal/mol) of the best pose for each ligand and macromolecule selected upon visual evaluation was noted.

3. Results and discussion

3.1. *Cytotoxicity and supercoiled pBR322 plasmid DNA hydrolytic cleavage experiments*

Chrysosplenetin inhibited proliferation of MCF-7 cells with an IC_{50} value of 0.3 µM after 72 hours treatment. Cytotoxicity of chrysosplenetin was evaluated for different treatment times. Sinha et al. treated some cancer cell lines MCF-7, HeLa, A549, HEK, T47D as well as a healthy cell line, HUVEC for 48 hours and found IC_{50} values as 4.2, 53.0, 45.0, 48.0, 6.2 and 100 µM, respectively [8]. After 24 hours treatment, chrysosplenetin inhibited proliferations of MDA-MB-23 and HT-29 with IC_{50} values of 235.0 and 310.0 µM [9]. Our finding is consistent with references.

In order to evaluate DNA damaging potential of chrysosplenetin, the supercoiled pBR322 plasmid DNA hydrolytic cleavage products were analyzed using agarose gel electrophoresis. A hydrolytic cleavage experiment was performed to evaluate the ability of the compound to damage the phosphodiester bonds of supercoiled pBR322 plasmid DNA. In general, pBR322 plasmid DNA has three forms in agarose gel electrophoresis. The supercoiled form, which is described as Form I, moves fast in the gel. Cleavage of one of the two strands gives the nicked form, described as Form II, which moves slower in the gel. If both strands are broken, the linear form of the plasmid, Form III, will be generated, which moves in between Form I and II [45]. As seen in **Figure 1**, presence of chrysosplenetin did not result in DNA cleavage at increasing concentrations (12.5, 25, 50, 100 and 200 µM) since Form I did not change to Form II and III in **lane 2-6**, i.e. chrysosplenetin did not damage the supercoiled pBR322 plasmid DNA under our experimental conditions.

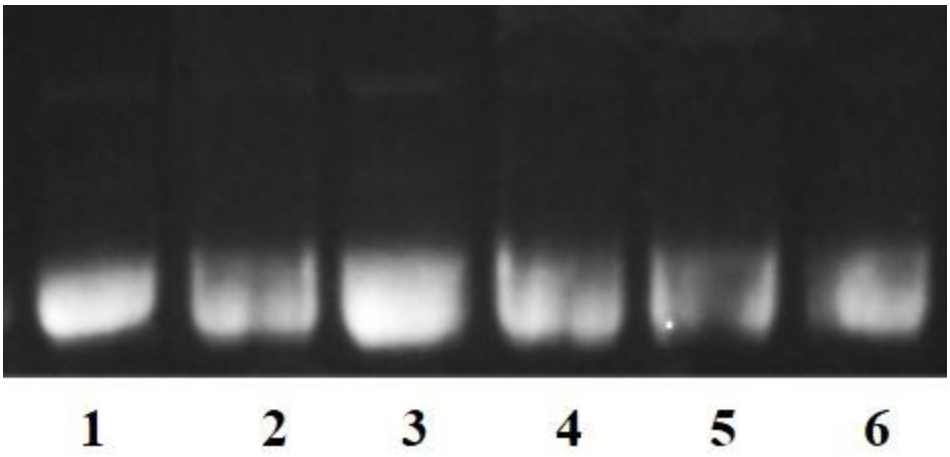

Figure 1. Supercoiled pBR322 plasmid DNA hydrolytic cleavage effect of chrysosplenetin. Lane 1, DNA control; lane 2-6, DNA+ chrysosplenetin (12.5 μM-25 μM-50 μM-100 μM-200 μM).

3.2. *Supercoiled pBR322 plasmid DNA protective experiments*

In order to investigate the protective effects of chrysosplenetin against oxidative damage to the supercoiled pBR322 plasmid DNA by hydroxyl radicals, we used agarose gel electrophoresis and Fenton reaction, which was started by $FeSO_4$ and H_2O_2 [46]. The results presented in **Figure 2** show that, in absence of chrysosplenetin, Form I disappeared completely, Form II and III were observed as 100% due to the DNA damage caused by hydroxyl radicals generated via Fenton reaction (**Figure 2**, lane 2). As shown on lane 3-6 in **Figure 2**, chrysosplenetin inhibited Fenton-induced damage of supercoiled pBR322 plasmid DNA in a concentration-dependent manner, which was evident by increasing intensities of Form I coinciding with increasing concentrations of chrysosplenetin (12.5, 25, 50 and 100 μM). The band intensities of Form I were found as 27.5%, 28.2%, 73.9% and 78.7%, respectively. In conclusion, chrysosplenetin protects DNA from oxidative damage, probably due to its radical scavenging properties [47].

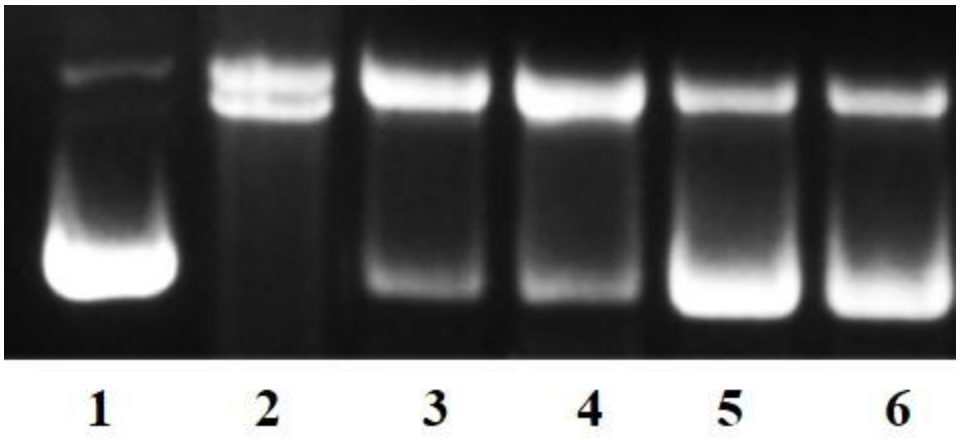

Figure 2. Supercoiled pBR322 plasmid DNA protective effects of chrysosplenetin. Lane 1: DNA control; lane 2: DNA + 1 mM $FeSO_4$ + 2% H_2O_2 bant 3-6: DNA + 1 mM $FeSO_4$ + 2% H_2O_2 + chrysosplenetin (12.5 µM-25 µM-50 µM-100 µM).

3.3. Topoisomerase I and II inhibition assay

The effects of chrysosplenetin on topoisomerase I and II were investigated using agarose gel electrophoresis. As shown in **Figure 3** and **Figure 4** (lane 2), when supercoiled pBR322 plasmid DNA was incubated with topoisomerases, Form I changed to Form II and Form III. For topoisomerase I, band intensities of Form I increased by 31.0%, 54.1%, 63.5% and 69.0% with increasing concentrations of chrysosplenetin (12.5, 25, 50 and 100 µM) and band intensities of Form II and III decreased. These results show that chrysosplenetin inhibits topoisomerase I in a concentration-dependent manner. In addition, chrysosplenetin showed remarkable inhibitory effect against topoisomerase II. The percentages of Form I were determined as 83.5%, 86.4%, 95.6% and 96.9%, respectively. All of these results demonstrate that chrysosplenetin has dual inhibitory effect against topoisomerase I and II. In several previous studies, flavonoids have been shown to inhibit topoisomerases. Quercetin and apigenin did not inhibit topoisomerase I-DNA complexes in K562

cells whereas they were found to moderately inhibit topoisomerase II. Fisetin and myricetin reportedly behaved as dual inhibitors of topoisomerase I and II [48]. Some flavonols, quercetin, kaempferol, fisetin, and myricetin were reported to inhibit topoisomerase II with IC_{50} values of 19.9, 28.0, 28.0, 34.6 µM respectively[49]. Moreover, topoisomerase I bioassay guided isolation studies on *Paphiopedilum callosum* (Rchb.f.) Stein led to isolation of some stilbenoids and two flavonoids, galangin and galangin-3-methylether [50]. Topoisomerase I inhibitory effect of galangin (range 0.2 -1.2 mM), associated with induction of Topoisomerase I conformation change and enhancement of the content of α-helix was also reported in other study [51].

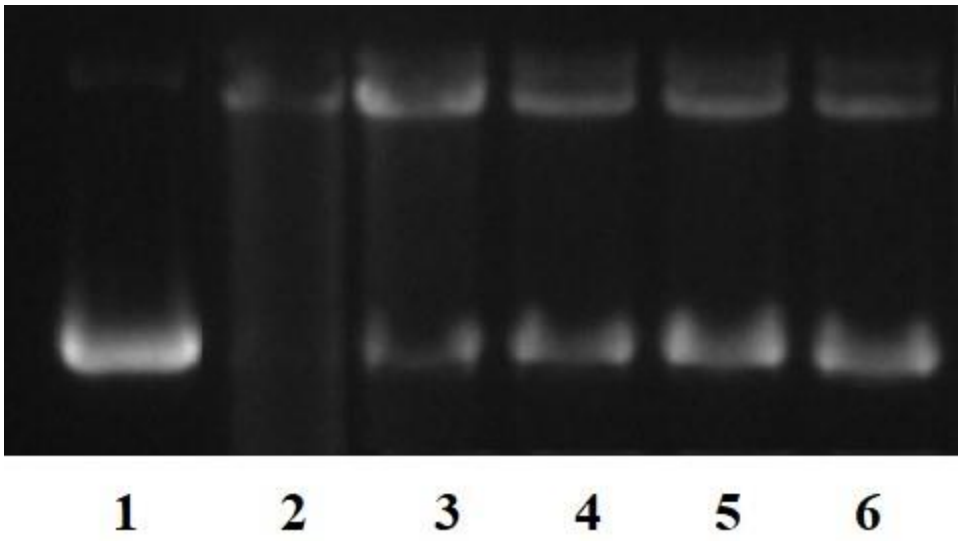

Figure 3. Topoisomerase I inhibitory effect of chrysosplenetin. Lane 1: DNA control; lane 2: DNA + 1 U topoisomerase I; lane 3-6: DNA + 1 U topoisomerase I + (chrysosplenetin (12.5, 25, 50, 100 µM)).

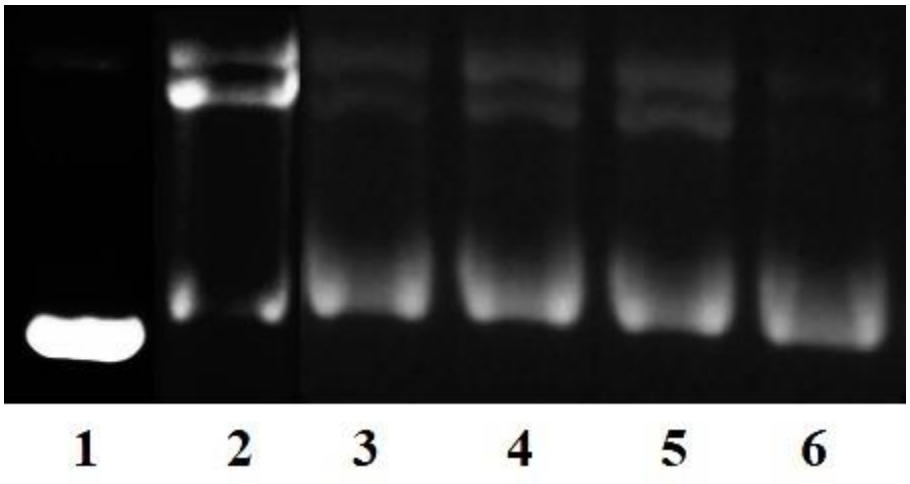

Figure 4. Topoisomerase II inhibitory effect of chrysosplenetin. Lane 1: DNA control; lane 2: DNA + 1 U topoisomerase II; lane 3-6: DNA + 1 U topoisomerase II + (chrysosplenetin (12.5, 25, 50, 100 μM)).

3.4. Molecular docking studies

3.4.1. Macromolecule selection and validation of the docking process

DNA damage through directly targeting DNA molecules is one of the most common strategies for designing antiproliferative agents. However, proteins protecting DNA from oxidative damage, such as DNA-binding protein Dps, and small molecules helping DNA repair, such as flavonoids, are known to bind to DNA [52, 53]. Small molecules can interact with DNA through intercalation, i.e. binding in between base pairs, or through groove binding, i.e. interacting with the minor and major grooves, which are rich with H bond donor and acceptor groups [54]. Compounds with large planar groups such as berberine and daunomycin tend to intercalate in between base pairs and polar moieties further stabilize this mode via H-bond interactions with DNA base nitrogens. Flexible compounds such as distamycin and netropsin on the other hand, are prone to fit

Table 1. Structural and co-crystallized ligand information of the selected pdb structures.

PDB ID	Structure	Binding type of the co-crystallized ligand	Resolution (Å)	RMSD (Å)[a]
3AJK	DNA	groove binding	1.95	0.86
3OIE	DNA	groove binding	1.90	0.80
3UOU	DNA	groove binding	1.24	0.75
3U05	DNA	groove binding	1.27	0.69
4AH0	DNA	groove binding	1.20	1.22
4IJ0	DNA	groove binding	1.54	0.99
4U8B	DNA	groove binding	1.31	0.89
4U8C	DNA	groove binding	1.24	0.63
6AST	DNA	groove binding	NMR[b]	0.85
6GIM	DNA	groove binding	1.43	0.50
1N37	DNA	intercalation	NMR[b]	1.27
1Z3F	DNA	intercalation	1.50	2.51
2DES	DNA	intercalation	1.50	0.70
2MG8	DNA	intercalation	NMR[b]	1.10
3FT6	DNA	intercalation	1.12	1.89
4BZT	DNA	intercalation	NMR[b]	0.77
182D	DNA	intercalation	1.80	0.54
198D	DNA	intercalation	1.97	0.73
224D	DNA	intercalation	1.40	0.64
367D	DNA	threading intercalation	1.20	1.76
1K4T	Topo I	intercalation	2.10	0.76
3QX3	Topo II	intercalation	2.16	0.51

[a] RMSD value of the docked conformer of the co-crystallized ligand regarding its original conformer.

[b] Structure resolved through solution NMR.

in grooves. Especially minor groove, which has a narrow gorge is quite suitable for flexible small molecules rather than large molecules like peptides and proteins [55]. Compounds featuring both large planar and flexible groups, such as nogalamycin can both intercalate in between base pairs and interact with the grooves, called threading intercalators [56]. Since the binding of a co-crystallized ligand may affect the results of chrysosplenetin docking, we selected 21 DNA structures from the Protein Data Bank, which include co-crystallized ligands with different binding types. Those resolved through X-ray crystallography were of 2.0 Å resolution or lower. The co-crystallized ligand of each DNA molecule was redocked and the RMSD value of the docked ligand was calculated regarding the co-crystallized conformation. All the structures, except 1Z3F, yielded low RMSD values (**Table 1**). 1Z3F was discarded and chrysosplenetin was docked to the remaining 20 DNA molecules. In the case of Topoisomerase I (1K4T) and II (3QX3) the RMSD of the co-crystallized ligands were excellent (**Table 1**).

3.4.2. Chrysosplenetin's binding to the DNA structures

Chrysosplenetin is composed of a 4-chromone ring to which a phenyl ring is attached at the 2nd position. The compound also has a number of methoxy and hydroxy substituents. Thus, with limited flexibility, planarity, and several H-bond donor and acceptor groups, chrysosplenetin was expected to display intercalation where possible and minor groove binding where intercalation is not possible. According to the results, this expectation was realized; chrysosplenetin showed intercalation with the structures having an intercalator co-crystallized ligand. For other structures it showed minor groove binding. 2KY7, however was an exception, with which chrysosplenetin interacted through groove binding although intercalation was possible (**Figure 5 A-C**). The 4-

chromone ring intensely engaged in π-π interactions in intercalation mode, while the hydroxyl groups made H bonds with the phosphate groups while binding to the groove (**Figure 5 D-F**) (See Supporting Information for more details.). The ability of chrysosplenetin to bind in both ways was also evident with the docking scores (**Table 2**). Docking score of chrysosplenetin was similar in most of the structures (within -6.5 and -7.5 kcal/mol range) although binding types were different. The scores also demonstrated that chrysosplenetin showed mild affinity to DNA compared to the tight binding co-crystallized ligands.

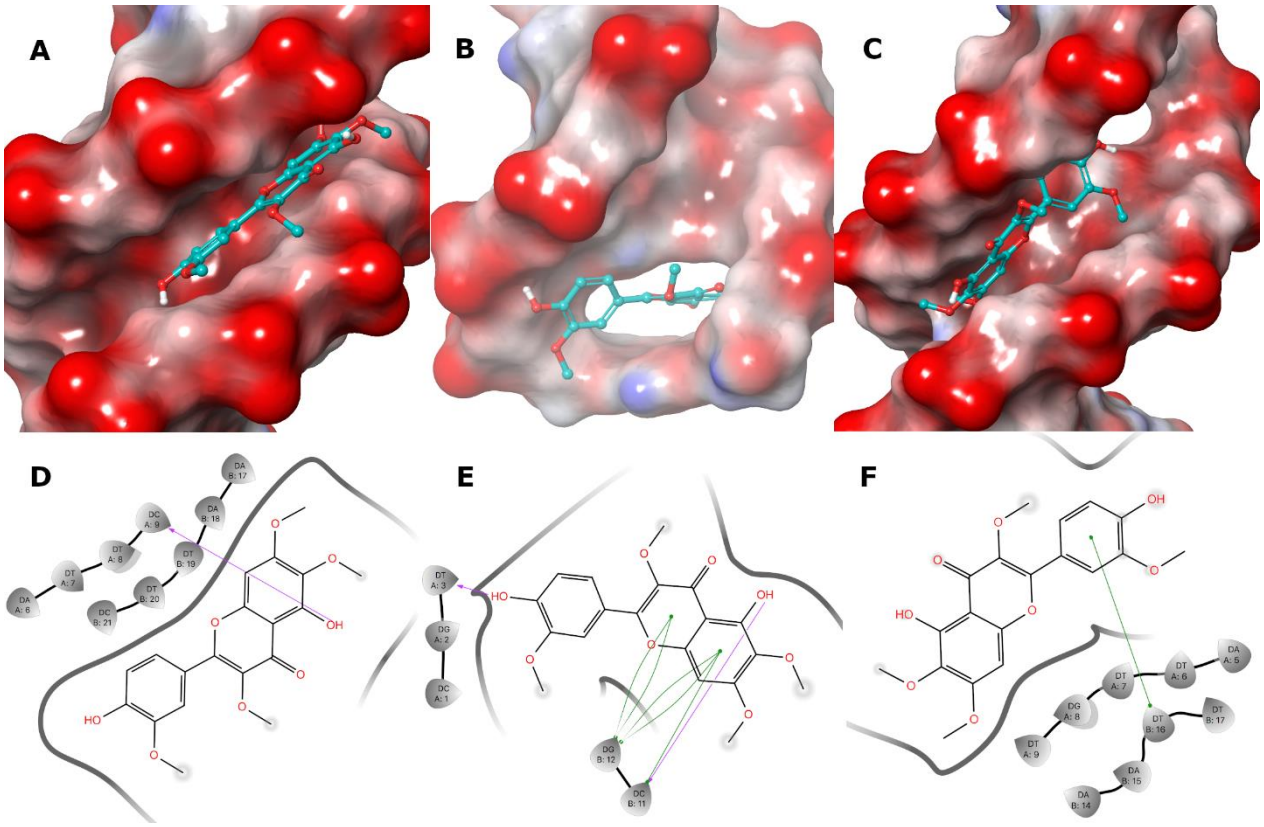

Figure 5. Binding modes (A-C) and interactions (D-F) of chrysosplenetin with 3OIE, 2DES, and 2KY7, respectively. Chrysosplenetin is represented as sticks and balls and the DNA molecules as molecular surface rendered according to the electrostatic potentials of the atoms with color ramp red-white-blue, in which red represents the lowest and blue represents the highest potential.

Table 2. Docking scores and binding types of chrysosplenetin with the DNA structures

PDB ID	Score (kcal/mol)		Binding type
	Chrysosplenetin	Co-crystallized ligand	
3AJK	-7.8	-12.3	groove binding
3OIE	-7.4	-17.3	groove binding
3U0U	-7.6	-12.0	groove binding
3U05	-7.5	-13.9	groove binding
4AH0	-7.6	-11.2	groove binding
4IJ0	-7.9	-14.1	groove binding
4U8B	-7.8	-15.4	groove binding
4U8C	-7.9	-17.5	groove binding
6AST	-6.8	-9.7	groove binding
6GIM	-7.3	-12.5	groove binding
1N37	-6.1	-7.7	intercalation
2DES	-6.8	-11.9	intercalation
2MG8	-5.9	-10.9	intercalation
3FT6	-8.8	-8.0	intercalation
4BZT	-8.4	-14.0	intercalation
182D	-7.1	-11.0	intercalation
198D	-6.6	-10.9	intercalation
224D	-7.0	-9.7	intercalation
367D	-8.2	-9.4	intercalation
2KY7	-6.7	-11.9	groove binding

3.4.3. Chrysosplenetin's binding to the DNA topoisomerases

The topoisomerase I structure used in this study (1K4T) is a covalent enzyme-DNA transient complex state in which the phosphodiester bond is broken at one strand of the DNA and a 3'-phosphotyrosyl intermediate is formed via Tyr723, instead. The co-crystallized ligand, topotecan, binds to the covalent complex by intercalating at the site of DNA cleavage making π-π stacking with both base pairs. Topotecan also makes direct and water-mediated H bonds with the enzyme Asp533, Asn722, and Tyr723 [42]. The topoisomerase II (3QX3) is also a covalent enzyme-DNA transient complex with two identical catalytic sites and in each site either strand of DNA is cut and one etoposide is bound. In Topoisomerase II, Tyr821 is engaged in phosphotyrosyl linkage in each cleavage site. In this structure, etoposide intercalates in between the base pairs in the cleavage site via its polycyclic aglycone core, while, being flexible unlike topotecan, its glycosidic and 4-hydroxy-3,5-dimethoxyphenyl groups stretch towards DNA major and minor grooves. Amino acids Gly478, Asp479, Leu502, Arg503, Gln778 and Met782 of the enzyme, as well as bases C14, G13, and T9 are the residues that etoposide interacts with. Topoisomerase poisons, such as topotecan and etoposide, tightly bind to and stabilize topoisomerase-DNA transient complexes thus prevent reattachment of the broken DNA strands by topoisomerase, which renders the DNA nonfunctional [57].

Although not as strong as topotecan and etoposide, chrysosplenetin bound to both enzyme-DNA complexes with fair affinity (**Table 3**). In topoisomerase I active site, chrysosplenetin was observed to intercalate at the DNA cleavage site in a very similar manner as topotecan (**Figure 6**). In this binding mode the 4-chromone and benzene rings made intense π-π interactions with one of the base pairs (A113 and T10), while H-bonds were formed with Arg364 and Asn722. The compound also bound to topoisomerase II in very similar way with π-π stacks with G13 base

through the 4-chromone ring and H-bond interactions with Arg503 and Gln778 (**Figure 6**) (See Supporting Information for more details.).

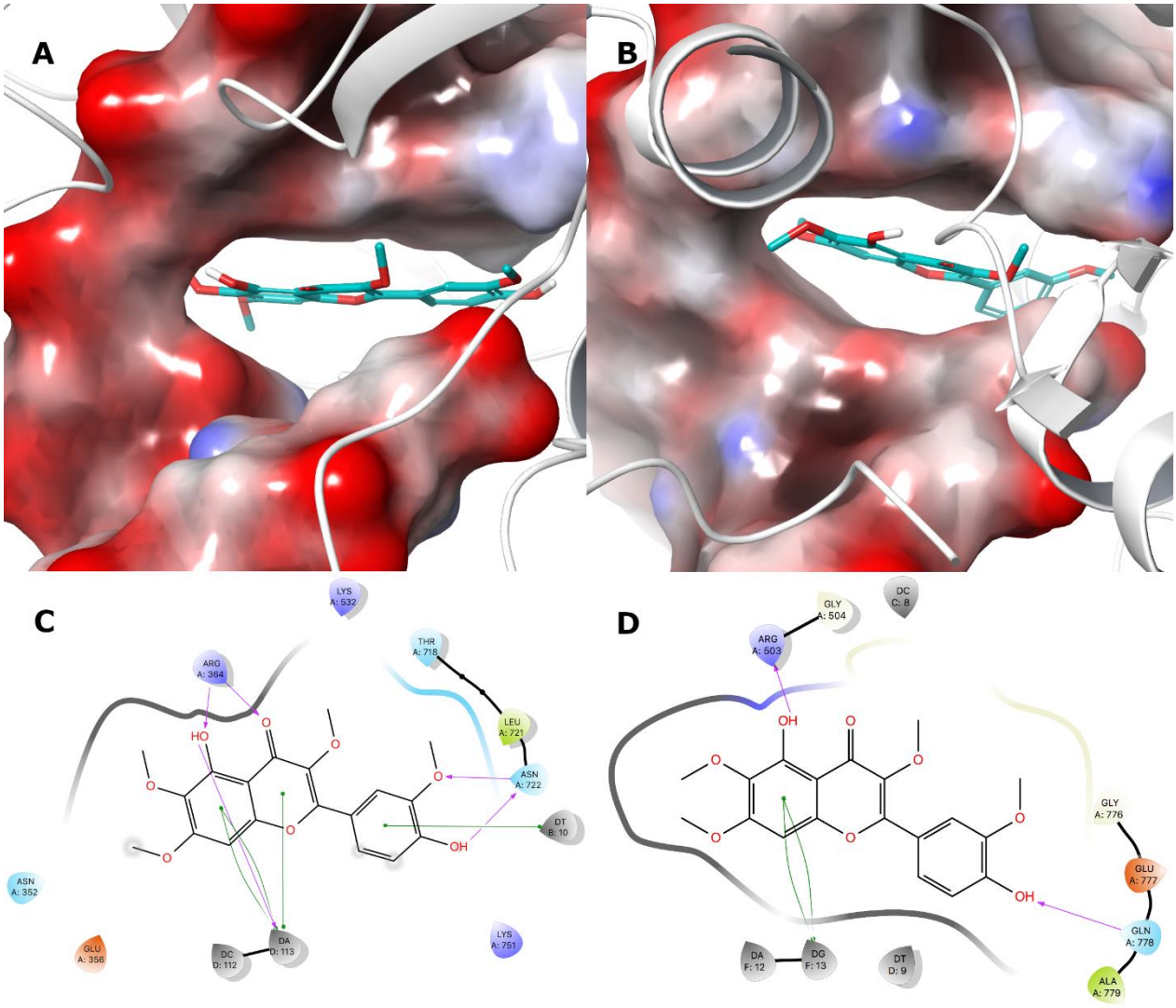

Figure 6. Binding modes (A, B) and interactions (C, D) of chrysosplenetin with covalent DNA complexes of topoisomerase I and II, respectively. Chrysosplenetin is represented as sticks, enzyme backbone as ribbons, and the DNA molecules as molecular surface rendered according to the electrostatic potentials of the atoms with color ramp red-white-blue, in which red represents the lowest and blue represents the highest potential.

Table 3. Docking scores (kcal/mol) of chrysosplenetin and the co-crystallized ligands with topoisomerases

Structure	Chrysosplenetin	Co-crystallized ligand
Topoisomerase 1	-9.1	-12.3
Topoisomerase II	-7.1	-12.1

Conclusions

In this study, we investigated DNA interaction, topoisomerase I and II inhibitory potentials of chrysosplenetin. The supercoiled pBR322 plasmid DNA hydrolytic cleavage, protective and topoisomerase I and II inhibitory effects were investigated using agarose gel electrophoresis. Chrysosplenetin did not show cleavage effects on increasing concentrations, therefore the results suggested that chrysosplenetin did not cause to damage of supercoiled pBR322 plasmid DNA. In addition, chrysosplenetin inhibited supercoiled pBR322 plasmid DNA damage induced by Fenton reactions in a concentration-dependent manner. All of topoisomerase I and II results showed that chrysosplenetin behaved as dual inhibitory effect on these enzymes, which may explain the cytotoxic effect of chrysosplenetin.

Molecular docking studies yielded results in line with the *in vitro* studies. Although not very tight, chrysosplenetin was predicted to bind to DNA via either intercalation or minor groove binding. This moderate affinity to DNA may be the reason for its protective effect against oxidative damage similar to other reported flavonoids. Tight binding to DNA would probably result in DNA damage in a similar way observed with DNA-binding antiproliferative agents. Molecular docking highlighted the importance of the 4-chromone core and the hydroxyl and methoxy groups for

interacting with DNA. Similarly, these structures seem to play important roles for binding to both DNA-topoisomerase complexes, since the affinity of the compound to these complexes mainly results from intercalating in between the base pairs in the cleavage sites.

In summary, this study highlighted Topoisomerase I and II inhibitory effect, which might be another mechanism of anti-cancer activity of chrysosplenetin.

Conflict of interest

The authors have declared that these are no conflict of interest

Acknowledgements

This work was supported by Hacettepe University Scientific Research Projects Coordination Unit (Project number: THD-2018-17448).

References

[1] H.Q. Tang, J. Hu, L. Yang, R.X. Tan, Terpenoids and flavonoids from Artemisia species, Planta Med 66(4) (2000) 391-3.

[2] M. Repčák, V. Švehlíková, J. Imrich, K. Pihlaja, Jaceidin and chrysosplenetin chemotypes of *Chamomilla recutita* (L.) Rauschert, Biochemical Systematics and Ecology 27(7) (1999) 727-732.

[3] G. Hong, X. He, Y. Shen, X. Chen, F. Yang, P. Yang, F. Pang, X. Han, W. He, Q. Wei, Chrysosplenetin promotes osteoblastogenesis of bone marrow stromal cells via Wnt/beta-catenin pathway and enhances osteogenesis in estrogen deficiency-induced bone loss, Stem Cell Res Ther 10(1) (2019) 277.

[4] R.R.J. Arroo, S. Sari, B. Barut, A. Ozel, K.C. Ruparelia, D. Sohretoglu, Flavones as tyrosinase inhibitors: kinetic studies in vitro and in silico, Phytochem Anal (2020).

[5] Y. Cao, Y. Zang, X. Huang, Z. Cheng, Chemical constituents from *Artemisia rupestris* and their neuraminidase inhibitory activity, Nat Prod Res (2019) 1-8.

[6] A.A. Gokmen, H. Can, H. Kayalar, B. Pektas, S. Kaya, In vitro anti-*Trichomonas vaginalis* activity of Haplophyllum myrtifolium, J Infect Dev Ctries 13(3) (2019) 240-244.

[7] J.E. Lan, X.J. Li, X.F. Zhu, Z.L. Sun, J.M. He, M. Zloh, S. Gibbons, Q. Mu, Flavonoids from *Artemisia rupestris* and their synergistic antibacterial effects on drug-resistant Staphylococcus aureus, Natural Product Research (2019).

[8] M.-R. Delnavazi, P. Saiyarsarai, S. Jafari-Nodooshan, M. Khanavi, S. Tavakoli, H. Hadavinia, N. Yassa, Cytotoxic Flavonoids from the Aerial Parts of *Stachys lavandulifolia* Vahl, Pharm Sci 24(4) (2018) 332-339.

[9] S. Sinha, H. Amin, D. Nayak, M. Bhatnagar, P. Kacker, S. Chakraborty, S. Kitchlu, R. Vishwakarma, A. Goswami, S. Ghosal, Assessment of microtubule depolymerization property of

flavonoids isolated from *Tanacetum gracile* in breast cancer cells by biochemical and molecular docking approach, Chem Biol Interact 239 (2015) 1-11.

[10] A. Dehshahri, M. Ashrafizadeh, E. Ghasemipour Afshar, A. Pardakhty, A. Mandegary, R. Mohammadinejad, G. Sethi, Topoisomerase inhibitors: Pharmacology and emerging nanoscale delivery systems, Pharmacol Res 151 (2020) 104551.

[11] X. Liang, Q. Wu, S. Luan, Z. Yin, C. He, L. Yin, Y. Zou, Z. Yuan, L. Li, X. Song, M. He, C. Lv, W. Zhang, A comprehensive review of topoisomerase inhibitors as anticancer agents in the past decade, European Journal of Medicinal Chemistry 171 (2019) 129-168.

[12] K. Hevener, T.A. Verstak, K.E. Lutat, D.L. Riggsbee, J.W. Mooney, Recent developments in topoisomerase-targeted cancer chemotherapy, Acta Pharm Sin B 8(6) (2018) 844-861.

[13] D.B. Khadka, G.H. Tran, S. Shin, H.T. Nguyen, H.T. Cao, C. Zhao, Y. Jin, H.T. Van, M.V. Chau, Y. Kwon, T.N. Le, W.J. Cho, Substituted 2-arylquinazolinones: Design, synthesis, and evaluation of cytotoxicity and inhibition of topoisomerases, Eur J Med Chem 103 (2015) 69-79.

[14] Y. Pommier, Drugging topoisomerases: lessons and challenges, ACS Chem Biol 8(1) (2013) 82-95.

[15] D.F. Birt, S. Hendrich, W. Wang, Dietary agents in cancer prevention: flavonoids and isoflavonoids, Pharmacol Ther 90(2-3) (2001) 157-77.

[16] H.D. Woo, J. Kim, Dietary flavonoid intake and smoking-related cancer risk: a meta-analysis, PLoS One 8(9) (2013) e75604.

[17] M.S. Zheng, Y.K. Lee, Y. Li, K. Hwangbo, C.S. Lee, J.R. Kim, S.K. Lee, H.W. Chang, J.K. Son, Inhibition of DNA topoisomerases I and II and cytotoxicity of compounds from Ulmus davidiana var. japonica, Arch Pharm Res 33(9) (2010) 1307-15.

[18] D. Sohretoglu, C. Zhang, J. Luo, S. Huang, ReishiMax inhibits mTORC1/2 by activating AMPK and inhibiting IGFR/PI3K/Rheb in tumor cells, Signal Transduct Target Ther 4 (2019) 21.

[19] B. Barut, C.O. Yalcin, S. Sari, O. Coban, T. Keles, Z. Biyiklioglu, M. Abudayyak, U. Demirbas, A. Ozel, Novel water soluble BODIPY compounds: Synthesis, photochemical, DNA interaction, topoisomerases inhibition and photodynamic activity properties, Eur J Med Chem 183 (2019) 111685.

[20] B. Barut, E.N. Barut, S. Engin, A. Özel, F.S. Sezen, Investigation of the antioxidant, α-glucosidase inhibitory, anti-inflammatory, and DNA protective properties of *Vaccinium arctostaphylos* L, Turkish Journal of Pharmaceutical Sciences 16(2) (2019) 175-183.

[21] T. Keleş, B. Barut, A. Özel, Z. Biyiklioglu, Synthesis of water soluble silicon phthacyanine, naphthalocyanine bearing pyridine groups and investigation of their DNA interaction, topoisomerase inhibition, cytotoxic effects and cell cycle arrest properties, Dyes and Pigments 164 (2019) 372-383.

[22] E. Harder, W. Damm, J. Maple, C. Wu, M. Reboul, J.Y. Xiang, L. Wang, D. Lupyan, M.K. Dahlgren, J.L. Knight, J.W. Kaus, D.S. Cerutti, G. Krilov, W.L. Jorgensen, R. Abel, R.A. Friesner, OPLS3: A Force Field Providing Broad Coverage of Drug-like Small Molecules and Proteins, J Chem Theory Comput 12(1) (2016) 281-96.

[23] G.M. Morris, R. Huey, W. Lindstrom, M.F. Sanner, R.K. Belew, D.S. Goodsell, A.J. Olson, AutoDock4 and AutoDockTools4: Automated docking with selective receptor flexibility, J Comput Chem 30(16) (2009) 2785-91.

[24] M. Tsunoda, T. Sakaue, S. Naito, T. Sunami, N. Abe, Y. Ueno, A. Matsuda, A. Takenaka, Insights into the structures of DNA damaged by hydroxyl radical: crystal structures of DNA duplexes containing 5-formyluracil, J Nucleic Acids 2010 (2010) 107289.

[25] S.N. Lin, S.; Campbell, N., Crystal structure of the DB1880-D(CGCGAATTCGCG)2 complex, (2011).

[26] D. Wei, W.D. Wilson, S. Neidle, Small-molecule binding to the DNA minor groove is mediated by a conserved water cluster, J Am Chem Soc 135(4) (2013) 1369-77.

[27] D.G.M. Munnur, E. P.; Forsyth, V. T.; Teixeira, S. C. M.; Neidle, S., CRYSTAL STRUCTURE OF THE DB 985-D(CGCAAATTTGCG)2 COMPLEX AT 1.20 A RESOLUTION, (2013).

[28] F. Zhang, M. Tsunoda, K. Suzuki, Y. Kikuchi, O. Wilkinson, C.L. Millington, G.P. Margison, D.M. Williams, E. Czarina Morishita, A. Takenaka, Structures of DNA duplexes containing O6-carboxymethylguanine, a lesion associated with gastrointestinal cancer, reveal a mechanism for inducing pyrimidine transition mutations, Nucleic Acids Res 41(10) (2013) 5524-32.

[29] W. Zhu, Y. Wang, K. Li, J. Gao, C.H. Huang, C.C. Chen, T.P. Ko, Y. Zhang, R.T. Guo, E. Oldfield, Antibacterial drug leads: DNA and enzyme multitargeting, J Med Chem 58(3) (2015) 1215-27.

[30] N.K. Harika, M.W. Germann, W.D. Wilson, First Structure of a Designed Minor Groove Binding Heterocyclic Cation that Specifically Recognizes Mixed DNA Base Pair Sequences, Chemistry 23(69) (2017) 17612-17620.

[31] C.R. Millan, F.J. Acosta-Reyes, L. Lagartera, G.U. Ebiloma, L. Lemgruber, J.J. Nue Martinez, N. Saperas, C. Dardonville, H.P. de Koning, J.L. Campos, Functional and structural analysis of AT-specific minor groove binders that disrupt DNA-protein interactions and cause disintegration of the Trypanosoma brucei kinetoplast, Nucleic Acids Res 45(14) (2017) 8378-8391.

[32] M.S. Searle, A.J. Maynard, H.E. Williams, DNA recognition by the anthracycline antibiotic respinomycin D: NMR structure of the intercalation complex with d(AGACGTCT)2, Org Biomol Chem 1(1) (2003) 60-6.

[33] A. Canals, M. Purciolas, J. Aymami, M. Coll, The anticancer agent ellipticine unwinds DNA by intercalative binding in an orientation parallel to base pairs, Acta Crystallogr D Biol Crystallogr 61(Pt 7) (2005) 1009-12.

[34] M. Cirilli, F. Bachechi, G. Ughetto, F.P. Colonna, M.L. Capobianco, Interactions between morpholinyl anthracyclines and DNA. The crystal structure of a morpholino doxorubicin bound to d(CGTACG), J Mol Biol 230(3) (1993) 878-89.

[35] C. Lin, R.I. Mathad, Z. Zhang, N. Sidell, D. Yang, Solution structure of a 2:1 complex of anticancer drug XR5944 with TFF1 estrogen response element: insights into DNA recognition by a bis-intercalator, Nucleic Acids Res 42(9) (2014) 6012-24.

[36] T.P. Maehigashi, O.; Hud, N. V.; Williams, L. D., Crystal Structure of Proflavine in Complex with a DNA hexamer duplex, (2010).

[37] A. Serobian, D.S. Thomas, G.E. Ball, W.A. Denny, L.P. Wakelin, The solution structure of bis(phenazine-1-carboxamide)-DNA complexes: MLN 944 binding corrected and extended, Biopolymers 101(11) (2014) 1099-113.

[38] C.K. Smith, G.J. Davies, E.J. Dodson, M.H. Moore, DNA-nogalamycin interactions: the crystal structure of d(TGATCA) complexed with nogalamycin, Biochemistry 34(2) (1995) 415-25.

[39] A. Dautant, B. Langlois d'Estaintot, B. Gallois, T. Brown, W.N. Hunter, A trigonal form of the idarubicin:d(CGATCG) complex; crystal and molecular structure at 2.0 A resolution, Nucleic Acids Res 23(10) (1995) 1710-6.

[40] G.S. Schuerman, C.K. Smith, J.P. Turkenburg, A.N. Dettmar, L. Van Meervelt, M.H. Moore, DNA-drug refinement: a comparison of the programs NUCLSQ, PROLSQ, SHELXL93 and X-PLOR, using the low-temperature d(TGATCA)-nogalamycin structure, Acta Crystallogr D Biol Crystallogr 52(Pt 2) (1996) 299-314.

[41] A.K. Todd, A. Adams, J.H. Thorpe, W.A. Denny, L.P. Wakelin, C.J. Cardin, Major groove binding and 'DNA-induced' fit in the intercalation of a derivative of the mixed topoisomerase I/II poison N-(2-(dimethylamino)ethyl)acridine-4-carboxamide (DACA) into DNA: X-ray structure complexed to d(CG(5-BrU)ACG)2 at 1.3-A resolution, J Med Chem 42(4) (1999) 536-40.

[42] B.L. Staker, K. Hjerrild, M.D. Feese, C.A. Behnke, A.B. Burgin, Jr., L. Stewart, The mechanism of topoisomerase I poisoning by a camptothecin analog, Proc Natl Acad Sci U S A 99(24) (2002) 15387-92.

[43] C.C. Wu, T.K. Li, L. Farh, L.Y. Lin, T.S. Lin, Y.J. Yu, T.J. Yen, C.W. Chiang, N.L. Chan, Structural basis of type II topoisomerase inhibition by the anticancer drug etoposide, Science 333(6041) (2011) 459-62.

[44] H.M. Berman, J. Westbrook, Z. Feng, G. Gilliland, T.N. Bhat, H. Weissig, I.N. Shindyalov, P.E. Bourne, The Protein Data Bank, Nucleic Acids Res 28(1) (2000) 235-42.

[45] S. Eryilmaz, E. Turk Celikoglu, O. Idil, E. Inkaya, Z. Kozak, E. Misir, M. Gul, Derivatives of pyridine and thiazole hybrid: Synthesis, DFT, biological evaluation via antimicrobial and DNA cleavage activity, Bioorg Chem 95 (2020) 103476.

[46] S.Y. Yeung, W.H. Lan, C.S. Huang, C.P. Lin, C.P. Chan, M.C. Chang, J.H. Jeng, Scavenging property of three cresol isomers against H2O2, hypochlorite, superoxide and hydroxyl radicals, Food Chem Toxicol 40(10) (2002) 1403-13.

[47] E.G.E. Helal, N. Abou-Aouf, A.S.M. Khattab, A Possible Hypoglycemic and Antioxidant Effect of Herbal Mixture Extraction in Diabetic Rats, The Egyptian Journal of Hospital Medicine 58(1) (2015) 109-119.

[48] M. Lopez-Lazaro, E. Willmore, C.A. Austin, The dietary flavonoids myricetin and fisetin act as dual inhibitors of DNA topoisomerases I and II in cells, Mutat Res 696(1) (2010) 41-7.

[49] M. Esselen, S.W. Barth, Food-borne topoisomerase inhibitors: Risk or benefit, Advances in Molecular Toxicology, 2014, pp. 123-171.

[50] S.Y. Nwe, C. Tungphatthong, A. Laorpaksa, B. Sritularak, W. Thanakijcharoenpath, S. Tanasupawat, S. Sukrong, Bioassay-guided isolation of topoisomerase I poison from paphiopedilum callosum (Rchb.f.) stein, Records of Natural Products 14(2) (2019) 89-97.

[51] X. Zhao, J. Zhang, [Inhibitory effect of galangin on DNA topoisomerases in lung cancer cells], Zhong Nan Da Xue Xue Bao Yi Xue Ban 40(5) (2015) 479-85.

[52] A. Martinez, R. Kolter, Protection of DNA during oxidative stress by the nonspecific DNA-binding protein Dps, J Bacteriol 179(16) (1997) 5188-94.

[53] C.N. N'Soukpoe-Kossi, P. Bourassa, J.S. Mandeville, L. Bekale, H.A. Tajmir-Riahi, Structural modeling for DNA binding to antioxidants resveratrol, genistein and curcumin, J Photochem Photobiol B 151 (2015) 69-75.

[54] C.L. Kielkopf, S. White, J.W. Szewczyk, J.M. Turner, E.E. Baird, P.B. Dervan, D.C. Rees, A structural basis for recognition of A.T and T.A base pairs in the minor groove of B-DNA, Science 282(5386) (1998) 111-5.

[55] G.S. Khan, A. Shah, R. Zia ur, D. Barker, Chemistry of DNA minor groove binding agents, J Photochem Photobiol B 115 (2012) 105-18.

[56] T. Banerjee, S. Banerjee, S. Sett, S. Ghosh, T. Rakshit, R. Mukhopadhyay, Discriminating Intercalative Effects of Threading Intercalator Nogalamycin, from Classical Intercalator Daunomycin, Using Single Molecule Atomic Force Spectroscopy, PLoS One 11(5) (2016) e0154666.

[57] Y. Pommier, E. Leo, H. Zhang, C. Marchand, DNA topoisomerases and their poisoning by anticancer and antibacterial drugs, Chem Biol 17(5) (2010) 421-33.

SUPPORTING INFORMATION

In vitro and in silico assessment of DNA interaction, topoisomerase I and II inhibition properties of Chrysosplenetin

Didem Şöhretoğlua*, Burak Barutb, Suat Saric, Arzu Özelb,d, Randolph Arrooe

a Hacettepe University, Faculty of Pharmacy, Department of Pharmacognosy, Sıhhiye, Ankara, TR-06100, Ankara, Turkey

b Karadeniz Technical University, Faculty of Pharmacy, Department of Biochemistry, Trabzon, Turkey

c Hacettepe University, Faculty of Pharmacy, Department of Pharmaceutical Chemistry, Sıhhiye, Ankara, TR-06100, Ankara, Turkey

d Karadeniz Technical University, Drug and Pharmaceutical Technology Application and Research Center, Trabzon, Turkey

e De Montfort University, Leicester School of Pharmacy, The Gateway, Leicester, LE1 9BH, United Kingdom

*Corresponding author: didems@hacettepe.edu.tr

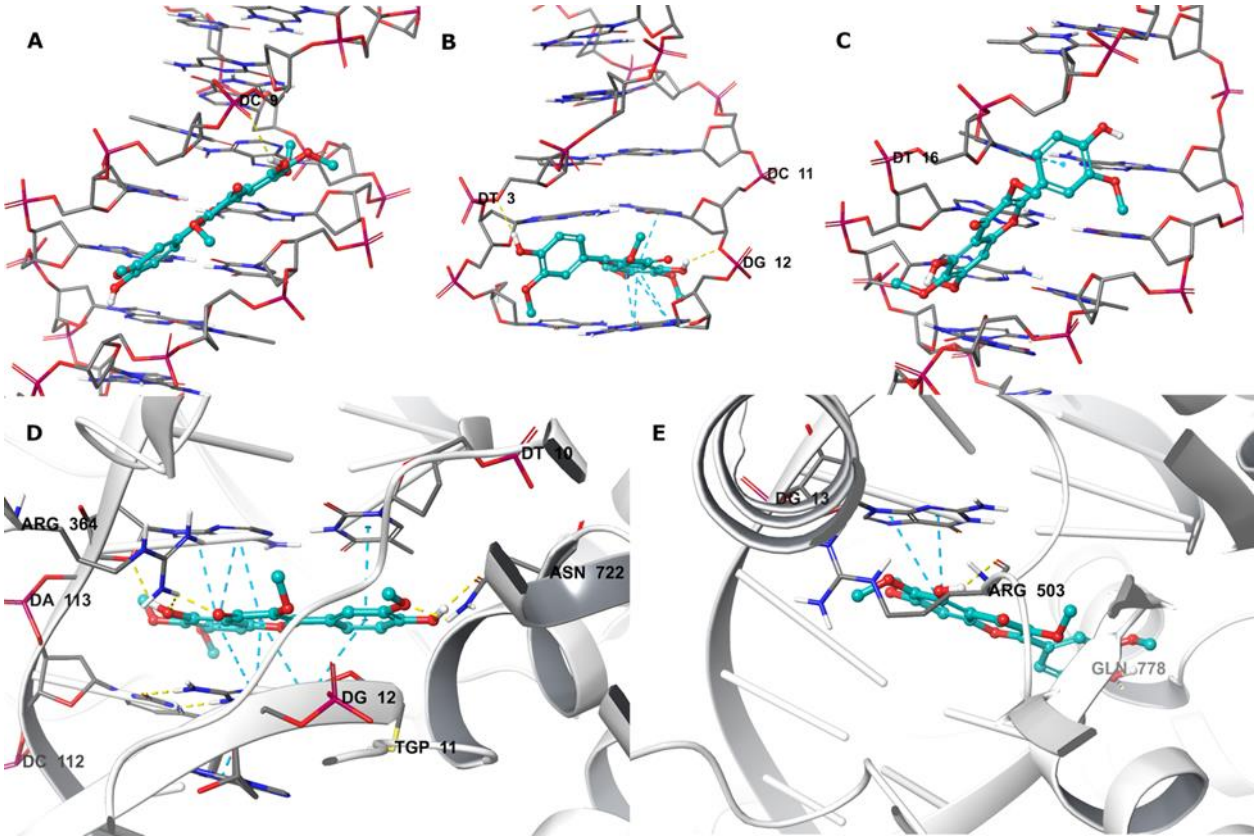

Figure S1. Binding interactions chrysosplenetin with 3OIE (A), 2DES (B), 2KY7 (C), 1K4T (D), and 3QX3 (E). Chrysosplenetin is represented as sticks and balls, H bond interactions as yellow dashes, π-π interactions as blue dashes, DNA molecules as sticks, and topoisomerase (with the DNA molecules) as ribbons.